# Chaac: Real-Time and Fine-Grained Rain Detection and Measurement Using Smartphones

Hansong Guo<sup>®</sup>, He Huang<sup>®</sup>, *Member, IEEE*, Yu-E Sun<sup>®</sup>, Youlin Zhang<sup>®</sup>, Shigang Chen<sup>®</sup>, *Fellow, IEEE*, and Liusheng Huang

Abstract—Rain observations with fine spatio-temporal granularity are significant for professional researches, decisionmaking, and our daily lives. However, the existing rain gauges can only cover less than 1% of the earth surface, and its amount is still decreasing. Even with the help of several other limited and immature supplementary techniques, rain observations today are still not precise enough. In such context, crowdsourcing paves the avenues toward a fault-tolerant rain observation network with unprecedented resolution and coverage, based on an alternative, nowadays omnipresent source, smartphones, which are integrated with abundant advanced sensors and are becoming more and more ubiquitous around us. In this paper, we propose Chaac, a novel system that exploits opportunistically crowdsourced audio clips from smartphone users to achieve precise detection and intensity measurement of rain. The evaluation results of performing Chaac on 1-s long audio segments demonstrate that it can detect and measure rain with 92.0% and 93.9% true positive rates, respectively.

*Index Terms*—Audio clips, crowdsourcing, rain detection and measurement, signal processing, smartphones, supervised classification.

# I. INTRODUCTION

## A. Professional Research and Decision-Making

THE DETECTION and intensity measurement of rain are crucial for many applications, such as weather prediction, water resources management, and agricultural production. Rain detection gives a result of whether it is raining currently and rain measurement reports a result of the current

Manuscript received April 1, 2018; revised July 8, 2018; accepted August 15, 2018. Date of publication August 22, 2018; date of current version February 25, 2019. This work was supported in part by the National Science Foundation under Grant NeTS 1718708, in part by the National Natural Science Foundation of China under Grant 61672369 and Grant 61572342, in part by the Natural Science Foundation of Jiangsu Province under Grant BK20161258, and in part by the Florida Cybersecurity Center. (Corresponding author: He Huang.)

- H. Guo is with the Department of Computer Science and Technology, University of Science and Technology of China, Hefei 230027, China, and also with the Department of Computer and Information Science and Engineering, University of Florida, Gainesville, FL 32611 USA (e-mail: guohanso@mail.ustc.edu.cn).
- H. Huang is with the School of Computer Science and Technology, Soochow University, Suzhou 215006, China (e-mail: huangh@suda.edu.cn).
- Y.-E Sun is with the School of Rail Transportation, Soochow University, Suzhou 215006, China (e-mail: sunye12@suda.edu.cn).
- Y. Zhang and S. Chen are with the Department of Computer and Information Science and Engineering, University of Florida, Gainesville, FL 32611 USA (e-mail: ylzh10@ufl.edu; sgchen@cise.ufl.edu).
- L. Huang is with the Department of Computer Science and Technology, University of Science and Technology of China, Hefei 230027, China (e-mail: lshuang@ustc.edu.cn).

Digital Object Identifier 10.1109/JIOT.2018.2866690

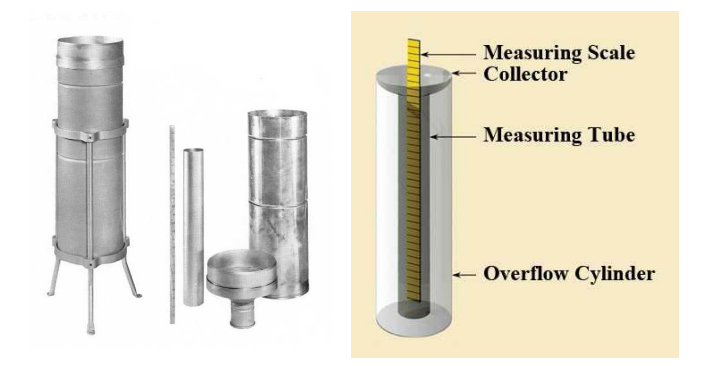


Fig. 1. Standard rain gauge and its components.

rain intensity. Rain gauges are essential tools for detecting and measuring rain, which have many drawbacks but still remain the de facto information source for hydrologic purpose. In Fig. 1, we present the standard rain gauge equipped by the National Oceanic and Atmospheric Administration in the U.S. on the left, and we detail its components on the right. Assume that every rain gauge can represent a surrounding region whose radius is 5 km. The Global Precipitation Climatology Centre has 67 000 available rain gauges, which still cannot cover 1% of the earth surface [16]. It is worth mentioning that 5 km is unrealistically large in describing the spatial variability of short-duration rain [33]. Moreover, the situation is getting worse as the number of rain gauges around the world is severely decreasing, both in developing and developed countries [39]. Weather radars are also important means to detect and measure rain, which, however, face numerous challenges, including anomalous propagation, amplification, attenuation or multiple reflection of the radar wave, and non-Rayleigh (i.e., too large) or nonmeteorological (e.g., mountains, aircraft, or birds) targets. In fact, a fine-grained and sufficient rain detecting and measuring method is in demand to serve as the calibration of weather radars.

#### B. Applications in Our Daily Lives

Precise rain information plays an essential role in our daily lives. For example, Miss. A is shopping in the mall. It is raining outside, but she does not take an umbrella with her. If the rain stops, she wants to know that immediately and seizes the opportunity to go home, because the rain may stop for a while and then restart at any time. In this case, the precise rain information can significantly benefit her. In fact, the weather apps

have become the most common way to acquire rain reports and forecasts. However, due to the imprecision of raw rain data that embodied in their coarse granularity of temporal and spatial resolution, the rain information released by existing weather apps is not always accurate. The inaccuracy in raw rain data mostly results from two factors. First, most cities only place a few rain gauges far away from the urban centers and record the rain data periodically. Second, the intensity of rain may changes dramatically with time and space. Therefore, it is hard to acquire raw observation data and provide accurate rain information even with the help of several other limited and immature supplementary methods. Later in Fig. 8, we will present the inaccuracy of rain information released by the China Meteorological Administration (CMA) and nine other favorite weather apps.

For traditional rain gauge-based rain detection and measurement sensor networks, except suffering from those limitations mentioned above, there is another challenge, that is, it is difficult to obtain real-time rain intensity data. The reasons are as follows. Rain intensity is the amount of rain per unit time, which nowadays is mainly measured by rain gauges. When we choose 10 or 30 min as time span to calculate the rain intensity, we find that the accumulated rain in rain gauge is too little to be precisely measured, especially for light rain. However, within this period of time, the rain intensity may have already changed several times.

Intuitively, we solve this problem by taking a different path, mobile sensing [14]. In recent years, a lot of not only excellent but also significant mobile sensing researches, which span a variety of areas, such as interaction [13], authentication [31], identification [41], recognition [38], privacy [18], [21], [22], localization [32], positioning [37], tracking [30], navigation [20], transportation [23], verification [34], assignment [36], monitoring [3], and make our lives more efficient, more intelligent, and more enjoyable. Yet, little attention has been paid to the field of rain observation. Mobile sensing will be applied to construct fault-tolerant rain monitoring networks, which will be real-time, fine-grained, and wide-coverage, based on an omnipresent source, smartphones, which are equipped with abundant advanced sensors and are becoming more and more pervasive in our daily lives. We now demonstrate the application of mobile sensing in realtime road condition monitoring with smartphone-based map apps [19]. Drivers open these map apps while driving on the road and then they are able to continuously receive real-time road condition information, including traffic congestion and sudden traffic accidents, ahead of them. Meanwhile, these map apps also collect and upload the drivers' locations and driving status, such as GPS positions, directions and speeds, using smartphone-equipped accelerometers and GPS. If there are many participants who use these map apps and share their own data, these map apps are even able to cover almost every geographical point and achieve extremely high accuracy. Compared to this approach, traditional sensor networks are sparsely deployed, mostly on main roads in cities, and are restricted by several limitations, including energy consumption, computing capability, etc. Therefore, these map apps can attain better performance than traditional sensor networks. Also, the construction of sensor networks incurs high costs, but these map apps take a different design path to utilize data shared by drivers for building real-time road condition monitoring systems at low costs.

In this paper, we develop Chaac which enables the participants to take part in the crowdsourcing process and report whether it is raining (as well as rain intensities) at their locations with audio clips from smartphones. Chaac can also cover almost every geographical point and achieve extremely high accuracy. To the best of our knowledge, this is the first work that can detect and measure the intensity of rain by smartphones, in both industrial and academic communities.

We summarize our main contributions as follows.

- We found that it is a practical and promising approach for real-time and fine-grained rain detection and measurement exploiting opportunistically crowdsourced audio clips from smartphones, among which the idea of employing the sound released by raindrops hitting on umbrella to measure the rain, is ingenious. The reason is that for traditional rain gauge-based rain detection and measurement sensor networks, it is difficult to obtain real-time and fine-grained rain information, especially rain intensity.
- 2) We implemented dozens of features [25] in frequency spectrum, time domain and power spectrum, and then carefully selected several of them, which are efficient in our application scenarios, according to extensive realworld experiments. Furthermore, we also created some very useful and low-cost features, which have never appeared in the literature before.
- 3) We put forward a novel method for describing the distribution of features extracted from different but continuous frames within a long time interval based on estimating a Gaussian mixture model (GMM), whose parameters are employed as new features for recognition.
- 4) We proposed a new system architecture for identifying surrounding environments, which is employed to recognize rain-related environments in this paper. If we select other appropriate features, our proposed system architecture can also be applied to identify a variety of other environments, such as thunder, wind, snow, etc. Previous researches in this area mainly paid attention to the recognition of human voices, and the sounds from surrounding environments were often treated as noises and processed at the very beginning. Our system architecture, to the best of our knowledge, first fuses features extracted from two different granularities of sounds, frames and segments. The purpose of this design is to study and depict the intrinsic characteristics of all kinds of sounds more subtly, and at the same time take calculation as well as energy consumption into consideration.
- 5) We implemented our system and evaluated it over six months period, during which we conducted extensive laborious experiments in the rain and collected massive amounts of valuable data. We will be very happy to share these data with later researchers for further studies in this area. The results demonstrated that our system is highly accurate and robust in detecting and measuring the rain,

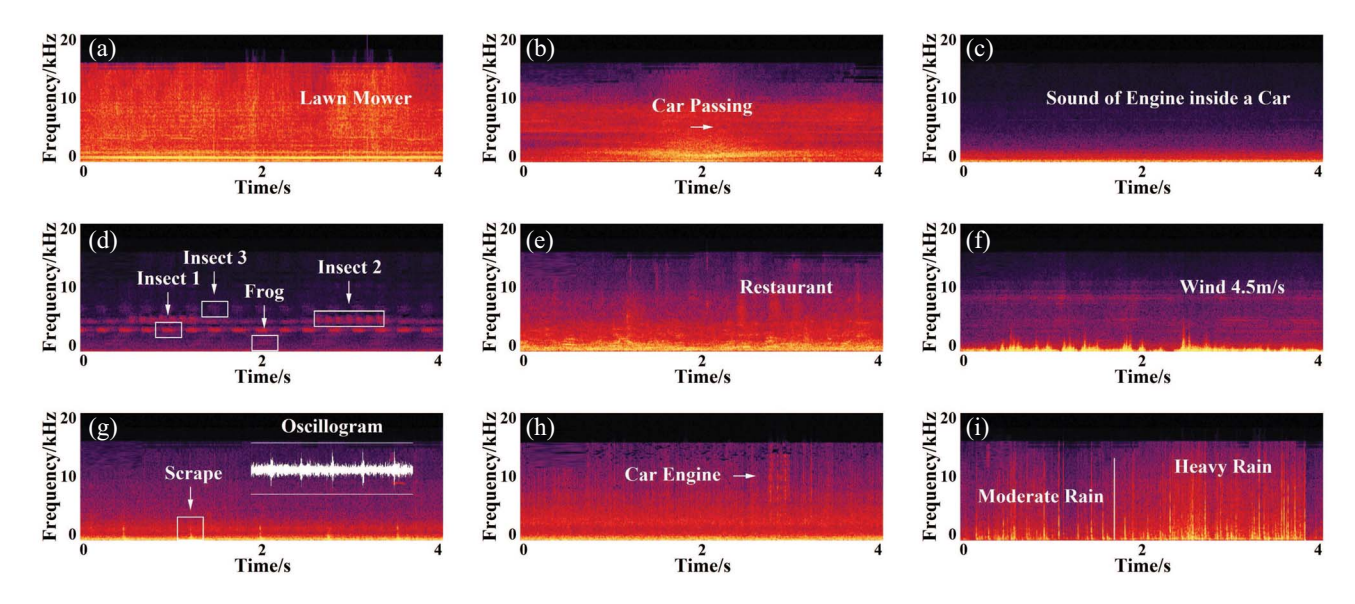


Fig. 2. Spectrograms of 4-s long audio segments which are crowdsourced from nine common scenes in our daily lives, including (a) lawn mower, (b) car passing, (c) sound of engine inside a car, (d) insects and a frog, (e) clamor of crowd in a restaurant, (f) wind, (g) scrapes of windshield wipers, (h) raindrops drumming against car window, and (i) raindrops drumming against umbrella.

whose performance is, to the best of our knowledge, superior to any other relevant existing approach, in both industrial and academic communities.

A spectrogram is a kind of visual spectrum representing the signal strength, of an audio segment, over time at various frequencies. A spectrogram basically consists of three dimensions, namely, the first dimension, the *x*-axis, which represents the time, the second dimension, the *y*-axis, which is on behalf of the frequency, as well as the third dimension, the color, which stands for the intensity (i.e., the amplitude of a particular frequency at a particular time). Specifically, dark colors correspond to small amplitudes and bright colors correspond to large amplitudes. Fig. 2 gives the spectrograms of 4-s long audio segments which are crowdsourced from nine common scenes in our daily lives.

The rest of this paper is organized as follows. Section II reviews the related work. Section III proposes the system overview. Section IV presents the system design and implementation. Section V describes the evaluation. Section VI gives the discussion. Finally, Section VII draws the conclusion.

## II. RELATED WORK

With regard to the rain detection and measurement, excluding two traditional techniques, that is, rain gauges and weather radars, the remaining relevant researches can be grouped into the following four categories.

#### A. Images-Based Work

Images are the most widely used method for rain detection. Allamano *et al.* [1] proposed a rain detection [29] presented an image registration and restoration system in rainy weather conditions, by detecting and eliminating the raindrops on images. To make intelligent wiper system possible, Görmer *et al.* [7] developed a rain detection system based on automotive in-vehicle cameras and introduced a false

activations avoidance mechanism. Focusing on the driving safety, Nashashibi *et al.* [24] conducted another similar research, namely, the detection of unfocused raindrops on windscreens using cameras. All of these researches are either smartphones-based or in-vehicle cameras-based. Compared with Chaac, the first category requires the participants to take photographs actively. This will weaken their intentions to participate in the crowdsourcing, because they have to accomplish extra tasks. On the contrary, Chaac can independently collect the audio clips from smartphones and do not need the help of the participants. And as for the second category, in-vehicle cameras, on the one hand, lack the capacity of processing these images, on the other hand, cannot transmit the images to the servers. So the rain detection results are not real-time.

## B. Wireless Links-Based Work

In some literatures, wireless links are also leveraged for rain detection. Leijnse *et al.* [17] investigated the potential of wireless links, for instance, employed by commercial companies for cellular communication, to detect the rain. The experiments using two 38-GHz links of eight rain events during two months in The Netherlands show that the appearances of these rain events can be well captured by the wireless links. Rayitsfeld *et al.* [26] explored the long term rain detection and measurement, leveraging the data from wireless links, interpolated at the locations of rain gauges nearby. Zinevich *et al.* [42] put forward the concept of recovering the rain dynamics employing the correlations of wireless links and made the observations assimilated into a stochastic temporal and spatial rain model. Compared with Chaac, wireless links-based rain detection systems are not fine-grained and cannot detect.

## C. Satellites-Based Work

In recent years, researchers exploited satellites for rain detection in a larger area. Bellerby et al. [2] designed a

rain detection system using the combination of rain radars and satellites by training an artificial neural network detector. Grimes and Diop [8] improved the satellites-based rain detection system by incorporating other weather information via a multiple regression. Wardah *et al.* [35] exploited the images from satellites and developed a rain detection system for flash flood warning. Compared with Chaac, these systems apparently, need the help of the satellites, which are expensive devices. And they will also spend enormous resources, such as energy and computing capability, to process these images. Moreover, the rain detection results of these systems are not fine-grained.

## D. Wipers-Based Work

There is another novel research, which is related to the rain detection. Haberlandt and Sester [10] studied the relationship between the speeds of vehicle wipers and the rain observations. They considered the vehicles as moving rain gauges and the wipers, to some extent, as sensors for rain detection. Compared with Chaac, due to the limited activity ranges of the vehicles, this kind of system can only detect the rain on the roads, so the results are not fine-grained. Different from these researches, Chaac avoided all of their disadvantages and achieved real-time and fine-grained rain detection and measurement leveraging the audio clips crowdsourced from smartphones. Meanwhile it is efficient, easy to be deployed, tasks-free for participants and does not require expensive devices.

#### III. SYSTEM OVERVIEW

The goal of our system is to achieve an ability to detect rain and measure rain intensity (if the rain detection result in the previous step shows that currently the sky is raining), both in real time (i.e., accurate to every point in time) and in fine granularity (i.e., accurate to every point in geography), using smartphones. The basic ideas behind our approach are as follows. When it rains, the rain will introduce special signatures in audio clips that our system collects from users' surroundings utilizing powerful sensors in smartphones. In Fig. 2, we give nine audio clips to visually show the clues of these signatures. Among all kinds of audio clips that are collected by our system in rainy days, those audio clips generated by raindrops hitting on umbrellas will have their own subtle but unique audio fingerprints. Moreover, focusing on this specific category of audio clips, rain with different intensities will produce different properties in these audio clips. Therefore, we can analyze the collected audio clips. First, we will detect whether these special rain-introduced signatures exist in the audio clips. Once these signatures are found in audio clips from a user's smartphone, we will know it is raining in this user's location at this moment. Then, we will recognize whether these subtle but unique raindrops hitting on umbrellas-generated audio fingerprints exist and try to extract them. Finally, we will distinguish those different properties produced by different intensities of the rain, among those collected audio clips. Once these audio fingerprints are captured and those properties are differentiated, we will be able to measure the rain intensity in this user's

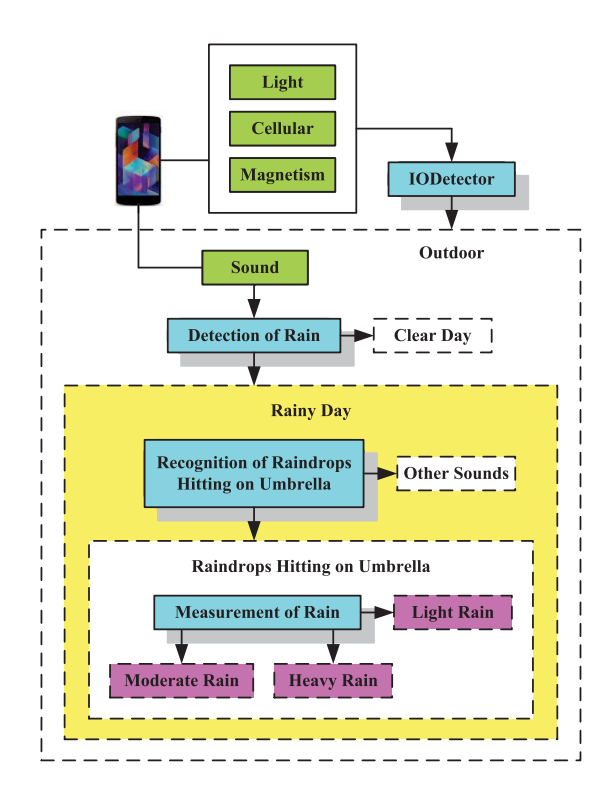


Fig. 3. System overview of Chaac.

location in real time. The challenges are as follows. On the one hand, in real life, the surroundings could be complicated, which will introduce interferences. These interferences make it difficult to detect the audio clips collected in rainy days and to ulteriorly recognize the audio clips generated by raindrops hitting on umbrellas, in all kinds of audio clips produced by other events in the surroundings. On the other hand, the differences among the properties produced by different intensities of the rain are small, which makes it difficult to precisely depict, mathematically model, quantitatively measure and eventually distinguish rain with different intensities. To address these challenges, we explore, propose, design, implement, and evaluate a brand new rain detection and measurement processing pipeline. The accuracy of our system is confirmed through a series of real-world experiments. Moreover, our solution for rain detection and measurement in this paper can be extended to many other application scenarios, such as the detection and measurement of snow, wind, thunder, and road sweeper.

In what follows, we provide the system overview of Chaac. To begin with, Chaac recognizes outdoor by using the IODetector proposed in [40], which is a smartphone-based system, synthetically leveraging light sensor, cellular sensor and magnetometer, for indoor and outdoor environment recognition. As shown in Fig. 3, Chaac contains three parts. The first part is the detection of rain. The details of this part will be given in Section IV-A. If it is raining, Chaac will try to ulteriorly judge whether the current audio clip is generated by raindrops hitting on umbrella. The details of this part will be presented in Section IV-B. If so, based on this type of audio clips, Chaac will measure current rain intensity in real time. The details of this part will be reported in Section IV-C.

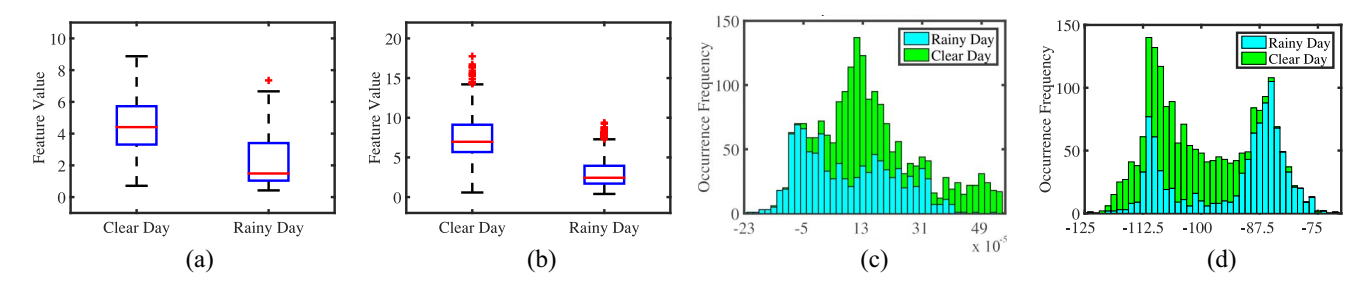


Fig. 4. In detection of rain. Box plots about RMSE-L, SS, and histograms about SD, AC-OF of 1000 rainy, and 1000 clear day segments. (a) Root mean squared error-low. (b) Spectral similarity. (c) Spectral decrease. (d) Amplitude of cut-off frequency.

Our proposed system can only detect and measure the falling (already existed) rain. It cannot forecast the rain or its intensity in advance.

#### IV. SYSTEM DESIGN AND IMPLEMENTATION

## A. Detection of Rain

In this section, we describe the four steps of detecting the rain. First, we collect raw audio clips from the smartphones. Second, the proposed system divides the raw clips into segments. Then our system conducts the feature extraction on the power spectrums of segments. At last, we construct a detector that makes judgments about whether a given segment is generated in a rainy day or sunny day.

- 1) Acquisition of Raw Audio Segments: We employ two popular segmentation methods, which are end-points detection and sliding windows, to divide audio clips into raw audio segments and set the length of every segment to 1 s.
- 2) Segment-Level Feature Extraction: The raw audio segments are not directly used in the recognition procedure. Instead, we consider the power spectrum of every segment, run feature extraction on the segments, and conduct the rain detection on the new features. In the following, we will introduce the extracted segment-level features (the details of extracted features can be referred in [9]).
- a) Min., med., and avg. amplitude: These features focus on the basic shape of power spectrum curve.
- b) Root mean squared error-low: This feature measures the smooth degree of power spectrum curve in low frequency part (i.e., less than 7500 Hz). The RMSE-L of segment  $S_i$  is calculated as<sup>1</sup>

$$RMSE-L_i = \sqrt{\frac{1}{nl_i^p} \sum_{j=1}^{nl_i^p} \left( d_{ij}^p - \tilde{a}_{ij}^p \right)^2}.$$

Fig. 4(a) presents the box plot with respect to RMSE-L of 1000 rainy day and 1000 clear day segments, respectively.

c) Spectral similarity: This feature describes the similarity between power spectrum curves in low and high frequency parts. The SS of segment  $S_i$  is calculated as

$$SS_i = \frac{1}{nl_i^p} \sum_{j=1}^{nl_i^p} |\hat{a}_{ij}^p - \hat{a}_{i(nl_i+j)}^p|.$$

 $^{1}$ In this paper, we use three superscripts p, t, and f to represent that a variable is calculated in power spectrum, time domain, and frequency spectrum.

Fig. 4(b) presents the box plot with respect to SS.

d) Spectral decrease: This feature weighs the decreasing degree of power spectrum curve. The SD of segment  $S_i$  is calculated as

$$SD_{i} = \frac{1}{\sum_{j=2}^{n_{i}^{p}} a_{ij}^{p}} \sum_{j=2}^{n_{i}^{p}} \frac{a_{ij}^{p} - a_{i1}^{p}}{j-1}$$

where  $n_i^p$  indicates the total number of frequency components in the power spectrum of segment  $S_i$ . Fig. 4(c) plots the histogram with respect to SD.

- *e)* Amplitude of middle frequency: This feature stands for the amplitude of 7500 Hz.
- *f)* Amplitude of cut-off frequency: This feature denotes the amplitude of 15 000 Hz. Fig. 4(d) plots the histogram with respect to AC-OF.
- 3) Construction of detector: Finally, Chaac constructs a detector, which outputs whether current audio segment is generated in rainy or sunny days. The details of this step will be given in Section V-A.
- 4) Transmission of refined audio clips: After the rain detection process, our system discards those audio clips which are identified as sunny days, and passes those audio clips which are marked as rainy days to the next computational process to ulteriorly recognize whether they are generated by raindrops hitting on umbrella.

## B. Recognition of Raindrops Hitting on Umbrella

As shown in Fig. 5, the proposed method takes seven steps to recognize raindrops hitting on the umbrella. Similar to Section IV-A, the proposed method first acquires audio clips from smartphones, then divide raw clips into segments. After that, we divide segments into frames and further conduct feature extraction for every frame. Given the extracted features of the frames with a segment, we construct the segment-level features by first accumulates the frame-level features and then perform the dimensional reduction on the accumulated features. At last, the proposed method builds a recognizer to judge whether the current audio segment is generated by raindrops hitting on the umbrella.

1) Segmentation of Segments Into Frames: In step three, in order to study and depict the characteristics of all kinds of sounds in rainy days more subtly, Chaac divides every segment

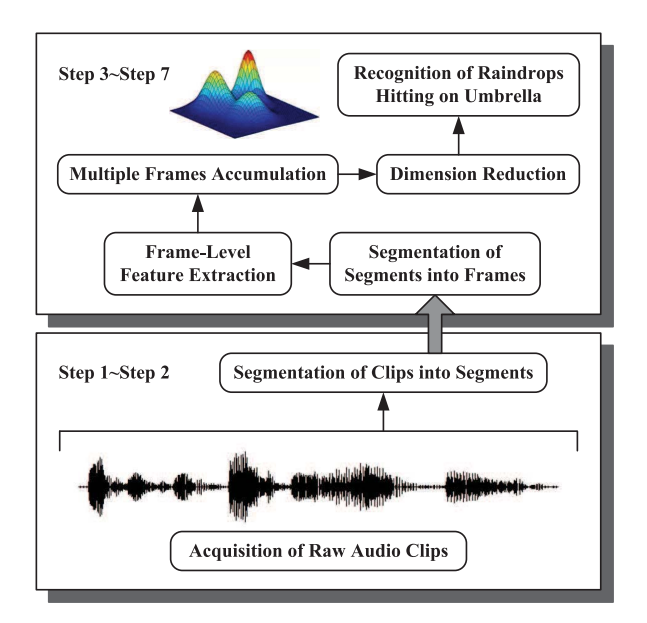


Fig. 5. In recognition of raindrops hitting on umbrella. Computational process.

into frames of equal length (0.032 s) and employ the Hanning window to overcome the frequency distortion problem.

- 2) Frame-Level Feature Extraction: Given the time domain and the frequency spectrum of the frames, we can perform frame-level feature extraction and further perform the recognition procedure on the extracted features. We now introduce some features used in classifying the sound of raindrops hitting on the umbrella.
- a) Avg. absolute amplitude: This feature describes the energy magnitude of audio signal in time domain. The AAA of frame  $F_i$  is calculated as

$$AAA_{i} = \frac{1}{n_{i}^{t}} \sum_{i=1}^{n_{i}^{t}} |s_{ij}^{t}|.$$

We also utilized some features described in [9] to identify the sound of raindrops. They are avg. zero-crossing rate, mel frequency cepstral coefficients, and spectral centroid.

b) Avg. zero-crossing rate: This feature counts the average number of occurrences that the sampling points of audio signal pass through the zero axis in time domain within a particular frame. The AZ-CR of frame  $F_i$  is calculated as

$$AZ-CR_{i} = \frac{1}{n_{i}^{t} - 1} \sum_{j=2}^{n_{i}^{t}} \left[ s_{ij}^{t} s_{i(j-1)}^{t} < 0 \right].$$

- c) Mel frequency cepstral coefficients: These features collectively represent the shape of the spectrum.
- d) Spectral centroid: This feature characterizes the barycenter of the frequency spectrum, which is correlated with the perceptual attribute of timbre, i.e., brightness. The SC of

frame  $F_i$  is calculated as

$$SC_{i} = \frac{\sum_{j=2}^{n_{i}^{f}} a_{ij}^{f} \log_{2} \frac{f_{ij}^{f}}{1000}}{\sum_{j=2}^{n_{i}^{f}} a_{ij}^{f}}.$$

3) Multiple Frames Accumulation: As mentioned before, in order to lucubrate the inherent properties of different sounds in rainy days, from smaller units. Chaac ulteriorly divides every segment into frames. However, during our experimental process, we find that frames are too transitory and features extracted from them cannot yield sufficient distinction degrees among different sounds. Thus, we first divide audio clips into segments which are the combinations of continuous frames. Then we conduct feature extraction for every segment by employing a GMM [27], [28], [43]. As described in Algorithm 1, we propose an EM-based algorithm to learn the parameters of GMM. The learned parameters are further regarded as the inputs of recognition procedure. There are two other benefits of our approach. First, it significantly reduces the scale of features for the first time, before feature dimension reduction, among all processing procedures. Second, it effectively avoids the influence of burst noises.

The GMM is able to approximate density distributions of arbitrary shapes smoothly. So we assume that the probability density function (PDF) of features extracted from frames within the *i*th segment can be represented as

$$PDF_i(f|\mu, \Sigma) = \sum_{i=1}^{n_{\text{gau}}} \alpha_j g(f|\mu_j, \Sigma_j)$$

where f indicates a d-dimensional feature vector, which is extracted from a frame within the ith segment.  $n_{\rm gau}$  indicates the total number of Gaussian PDFs (GPDFs) in every GMM.  $\alpha_j$  indicates the weight, namely, the magnitude, of the jth GPDF and the sum of all weights equals to 1. The jth GPDF is calculated as

$$g(f|\mu_j, \Sigma_j) = \frac{1}{\sqrt{(2\pi)^d |\Sigma_j|}} e^{-(f-\mu_j)^T \Sigma_j^{-1} (f-\mu_j)/2}$$

where  $\mu_j$  and  $\Sigma_j$  indicate the mean vector and covariance matrix, namely, the location and width, of the *j*th GPDF, respectively. In order to obtain the optimal parameter values of the GMM to describe these observed feature vectors, we employ maximum likelihood estimation and maximize the following log-likelihood function (LLF):

$$LLF_i = \log \left[ \prod_{k=1}^{n_{fra}} PDF_i(f_{ik}|\mu, \Sigma) \right]$$

where  $n_{\text{fra}}$  indicates the total number of frames in every segment.  $f_{ik}$  indicates features extracted from the kth frame within the ith segment. Generally, we assume that the covariance matrix of the jth GPDF can be represented as

$$\Sigma_j = \sigma_j^2 I$$

where  $\sigma_j^2$  indicates the variance vector of the *j*th GPDF. *I* indicates the identity matrix. Nevertheless, the LLF is nonlinear for GMM parameters (i.e.,  $\mu_j$ ,  $\sigma_j^2$ , and  $\alpha_j$ ), so the closed form solution to the problem of maximizing the aforesaid function does not exist. Consequently, we calculate the partial derivatives of the LLF with respect to  $\mu_j$  and  $\sigma_j^2$ , and then set their values equal to 0, respectively. The results are as follows:

$$\widetilde{\mu}_{j} = \frac{\sum\limits_{k=1}^{n_{\mathrm{fra}}} \beta_{j}(f_{ik})f_{ik}}{\sum\limits_{k=1}^{n_{\mathrm{fra}}} \beta_{j}(f_{ik})}$$

and

$$\widetilde{\sigma}_{j}^{2} = \frac{1}{d} \frac{\sum_{k=1}^{n_{\text{fra}}} \beta_{j}(f_{ik}) (f_{ik} - \widetilde{\mu}_{j})^{T} (f_{ik} - \widetilde{\mu}_{j})}{\sum_{k=1}^{n_{\text{fra}}} \beta_{j}(f_{ik})}$$

where  $\widetilde{\mu}_j$  and  $\widetilde{\sigma}_j^2$  indicate the re-estimation formulas of the mean and variance vectors, which will be utilized in iterative steps of our expectation maximization algorithm.  $\beta_j(f_{ik})$  is the posterior probability, which is calculated as

$$\beta_j(f_{ik}) = \frac{\alpha_j g(f_{ik}|\mu_j, \sigma_j^2)}{\text{PDF}_i(f_{ik}|\mu, \sigma^2)}.$$

Furthermore, we also calculate the partial derivative of the LLF with respect to  $\alpha_j$ , and then make its value equal to 0, under the constraint that the sum of all weights equals to 1 simultaneously. Therefore, we employ the Lagrange multiplier when solving these equations and the result is as follows:

$$\widetilde{\alpha}_j = \frac{1}{n_{\text{fra}}} \sum_{k=1}^{n_{\text{fra}}} \beta_j(f_{ik})$$

where  $\tilde{\alpha}_i$  indicates the re-estimation formula of the weight.

- 4) Dimension Reduction: The features output by GMM have 75 dimensions. In this paper, we integrate the linear discriminant analysis (LDA) into Chaac to reduce the dimension of features.
- 5) Construction of Recognizer: Finally, Chaac constructs a recognizer, which outputs whether current audio segment is generated by raindrops hitting on umbrella or other sources. The details of this step will be presented in Section V-B.
- 6) Transmission of Refined Audio Clips: After the raindrops hitting on umbrella recognition process, our system passes those audio clips which are marked as raindrops hitting on umbrella to the next computational process to eventually measure the intensity of the rain, and discards those audio clips which are identified as other sources.

#### C. Measurement of Rain

In this section, we provide the computational process of measuring the rain, which is similar to the rain detection. The first and second steps are acquiring audio clips from the previous computational process and then dividing them into segments. In the third step, our system extracts several

# Algorithm 1 Expectation Maximization

- 1: Input:
- 2:  $f_i$ :  $n_{fra}$  d-dimensional feature vectors, and each is extracted from a frame within the i-th segment.
- 3:  $n_{gau}$ : the total number of GPDFs employed in the GMM, whose value is 3.
- 4: *T*: the threshold parameter indicating the termination tolerance, whose value is 1e-6.
- 5:  $n_{iter}$ : the maximum number of iterations allowed, whose value is 1e3.
- 6: Output:
- 7:  $\mu$ ,  $\sigma^2$  and  $\alpha$ : the parameters of the GMM.
- 8: Initialization:
- conduct the k-Nearest Neighbors clustering on f<sub>i</sub> and divide them into n<sub>gau</sub> clusters;
- 10: **for** j **from** 1 **to**  $n_{gau}$  **do**
- 11:  $\mu_j$  = the mean vector of features within the *j*-th cluster;
- 12:  $\sigma_j^2$  = the covariance vector of features within the *j*-th cluster;
- 13:  $\alpha_j^J$  = the proportion of features within the *j*-th cluster in all features;

```
14: end for
15: \mu = [\mu_1, ..., \mu_{n_{gau}}]; \sigma^2 = [\sigma_1^2, ..., \sigma_{n_{gau}}^2]; \alpha = [\alpha_1, ..., \alpha_{n_{gau}}];

16: \theta = [\mu, \sigma^2, \alpha]; \widetilde{\theta} = [0, ..., 0]; t = 0;
 17: while t < n_{iter} do
                 for j from 1 to n_{gau} do
19:
                        Expectation Step:
                        calculate \beta_i;
20:
                        Maximization Step: calculate \widetilde{\mu}_j, \widetilde{\sigma}_i^2, \widetilde{\alpha}_j;
21:
22:
23:
                \widetilde{\mu} = [\widetilde{\mu}_1, ..., \widetilde{\mu}_{n_{gau}}]; \widetilde{\sigma}^2 = [\widetilde{\sigma}_1^2, ..., \widetilde{\sigma}_{n_{gau}}^2]; \widetilde{\alpha} = [\widetilde{\alpha}_1, ..., \widetilde{\alpha}_{n_{gau}}];
24:
                 \widetilde{\theta} = [\widetilde{\mu}, \, \widetilde{\sigma}^2, \, \widetilde{\alpha}];
25:
                 if \parallel \theta - \widetilde{\theta} \parallel < T then
26:
27:
                        break;
28:
                 end if
29:
                 \theta = \widetilde{\theta}; t = t + 1;
30: end while
```

segment-level features in power spectrum, which will be elaborated later in this section. Finally, our system constructs a measurer, which outputs the measurement results, namely, the rain intensity.

- 1) Segment-Level Feature Extraction: Here, we elaborate features which are selected to measure the rain. These features are all calculated in power spectrum of every segment.
- a) Max. amplitude: This feature focuses on the basic shape of every power spectrum curve. Fig. 6(a) presents the box plot with respect to MA of 700 light rain, 700 moderate rain, and 700 heavy rain segments in total.
- b) Energy-low: This feature pays attention to the signal energy in low frequency part. The E-L of segment  $S_i$  is calculated as

$$E-L_i = \sum_{j=1}^{nl_i^p} a_{ij}^p.$$

Fig. 6(b) presents the box plot with respect to E-L.

c) Spectral roll-off: This feature captures the frequency below which 75% of the signal energy is contained. The SR-O of segment  $S_i$  is calculated as

$$SR-O_i = \min j'$$

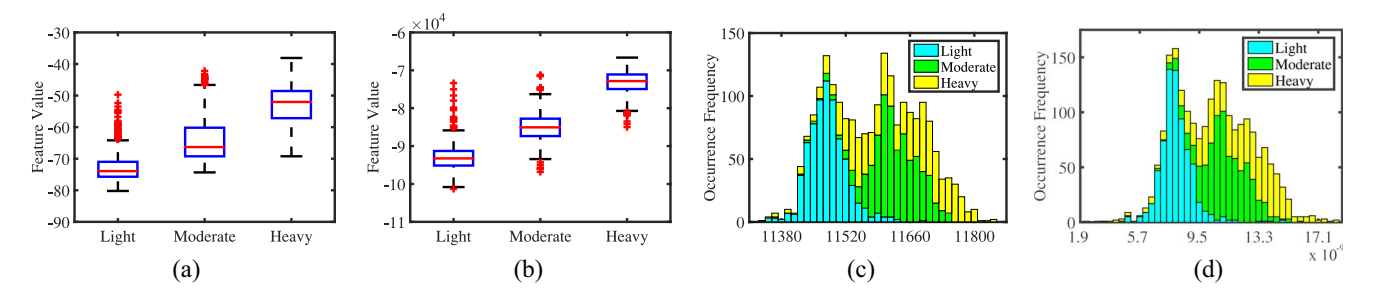


Fig. 6. In measurement of rain. Box plots about MA, E-L, and histograms about SR-O, SS of 700 light, 700 moderate, and 700 heavy rain segments. (a) Max. Amplitude. (b) Energy-low. (c) SpectralRoll-off. (d) SpectralSlope-measurement.

subject to

$$\sum_{j=1}^{j'} a_{ij}^p \ge 0.75 \sum_{j=1}^{n_i^p} a_{ij}^p.$$

Fig. 6(c) plots the histogram with respect to SR-O.

d) Spectral slope: This feature denotes the energy distribution at various frequencies. The SS of segment  $S_i$  is calculated as

$$SS_{i} = \frac{1}{\sum_{j=1}^{n_{i}^{p}} d_{ij}^{p} + \sum_{j=1}^{n_{i}^{p}} d_{ij}^{p} + \sum_{j=1}^{n_{i}^{p}} d_{ij}^{p} + \sum_{j=1}^{n_{i}^{p}} f_{ij}^{p}}{\sum_{j=1}^{n_{i}^{p}} d_{ij}^{p} + \sum_{j=1}^{n_{i}^{p}} (f_{ij}^{p})^{2} - \left(\sum_{j=1}^{n_{i}^{p}} f_{ij}^{p}\right)^{2}}.$$

Fig. 6(d) plots the histogram with respect to SS.

2) Construction of Measurer: Finally, Chaac constructs a measurer, which outputs the rain intensity. The details of the last step will be reported in Section V-C.

### V. EVALUATION

In this section, we present the results of our experiments. This section consists of four sections. In the first section, we demonstrate the experimental results of detecting the rain. In the following section, we study the experimental results of recognizing raindrops hitting on umbrella. Then we show the experimental results of measuring the rain, in the third section. Finally, we evaluate how well our system can detect and measure the rain in real world.

## A. Detection of Rain

In this section, we evaluate how well Chaac can detect the rain with the help of random forest (RF), which is an ensemble algorithm in machine learning and can be used for classification, regression, and other tasks. Our experimental dataset contains 7200 rainy day and 7200 clear day segments, respectively. RF is efficient on large-scale data, which can handle a large number of features, and does not over-fit. So in this paper, we choose RF to construct the rain-detector.

1) Experimental Results: We construct the detector based on RF. Then we conduct a series of tenfold cross-validation experiments on our dataset. Fig. 7 shows the confusion matrix, true positive rate (TPR) and false positive rate (FPR) of RF.

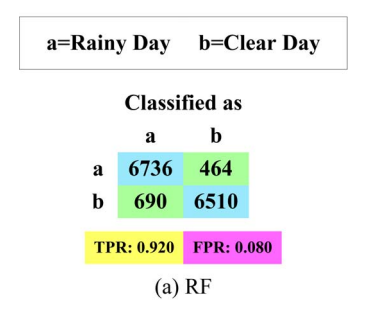


Fig. 7. In detection of rain. Confusion matrix, TPR, and FPR of RF.

The TPR is calculated as

$$TPR = \frac{n_{tp}}{n_{tp} + n_{fn}}$$

where  $n_{tp}$  indicates the total number of segments, whose classes are positive, and are correctly recognized by our proposed and trained system.  $n_{fn}$  indicates the total number of segments, whose classes are positive, but are wrongly recognized as negative by our proposed and trained system. The FPR is calculated as

$$FPR = \frac{n_{fp}}{n_{tn} + n_{fp}}$$

where  $n_{fp}$  indicates the total number of segments, whose classes are negative, but  $n_{tn}$  indicates the total number of segments, whose classes are negative. And are correctly recognized by our proposed and trained system.

We can observe that the RF achieves 92.0% TPR, 8.0% FPR, and 1154 misdetection segments.

2) Comparison With Existing Rain Detection Methods: Here, we demonstrate how well Chaac can detect the rain in real world. Chaac leverages the detection model constructed in the previous part, which is derived from 14 400 segments, and makes every decision based on ten consecutive segments. Fig. 8 illustrates the comparison among the rain detection results output by Chaac, the rain information released by the CMA and nine other popular weather apps. We mark the true detection results or information using cyan, and false employing red.

We can make three main observations here. First, the CMA misreports 12 times in a total of 21 sampling tests during three days and achieves 42.9% TPR. Second, with respect to all nine remaining weather apps, the average number of misreports and the average TPR released by every weather app are 10.1 times

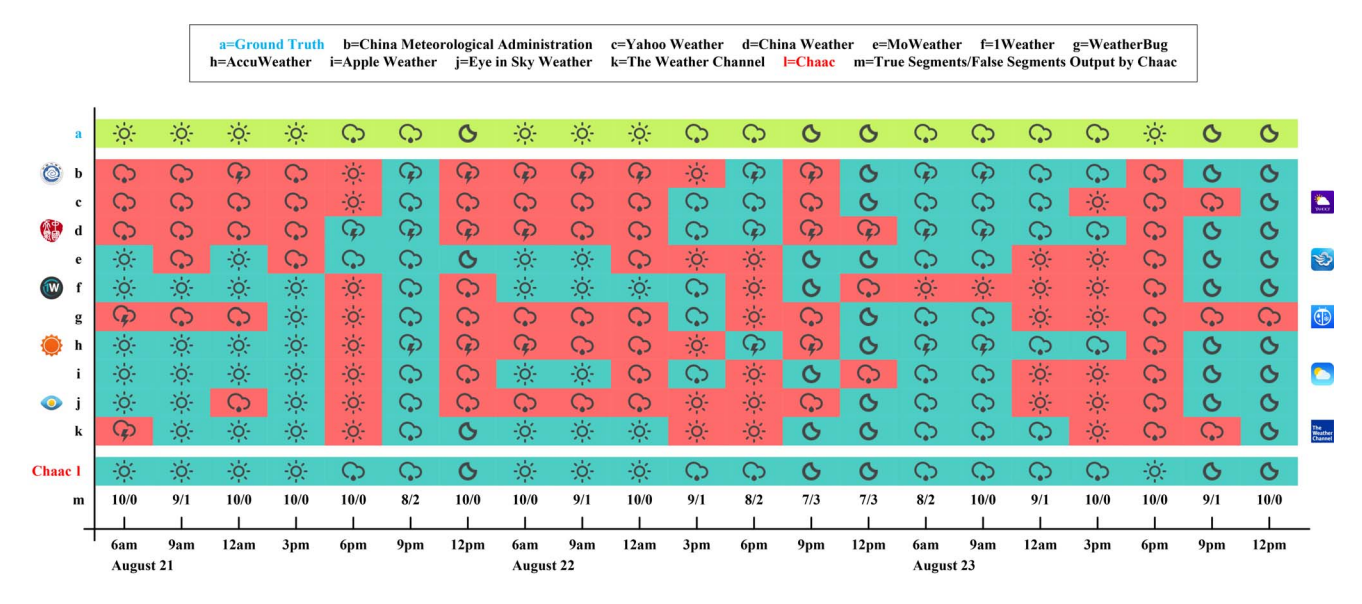


Fig. 8. In detection of rain. Comparison among the rain detection results output by Chaac, the rain information released by the CMA, and nine other popular weather apps, to show that Chaac works in real time.

and 51.9%, respectively. The Weather Channel yields the most accurate rain information, which only misreports seven times and achieves 66.7% TPR and the WeatherBug produces the most inaccurate rain information, which misreports 15 times and only achieves 28.6% TPR. Third, Chaac, our proposed system, can detect the rain with 100% TPR when deciding with ten consecutive segments, that is to say, Chaac will output rainy day as detection result, if the number of rainy day segments is greater than clear day segments among the detection results of these ten consecutive segments, and vice versa. Additionally, in row *m* of Fig. 8, we present the specific number of true and false detection results among ten consecutive segments output by Chaac in every sampling test.

#### B. Recognition of Raindrops Hitting on Umbrella

In this section, we present how well Chaac can recognize the segments generated by raindrops hitting on umbrella employing decision tree (DT), along with two different dimension reduction algorithms. Our experimental dataset contains 3600 segments generated by raindrops hitting on umbrella and 3600 other segments crowdsourced by the participants in rainy days, which are generated by all kinds of activities.

- 1) Time Consumption of Every Computational Step: In Table I, we show the average time consumption of our algorithm. The step-level time consumption is obtained by running the recognition experiments ten times and further computing the average time of every step. Apparently, the most time-consuming steps are segmentation of segments into frames and frame-level feature extraction. We also observe that the overall time of the recognition process for each segment is 88.51 ms.
- 2) Experimental Results: We construct the recognizer based on DT. In addition, we employ tenfold cross-validation to evaluate the performance of the recognizers when employing different dimensional reduction algorithms, respectively,

TABLE I
IN RECOGNITION OF RAINDROPS HITTING ON UMBRELLA.
TIME CONSUMPTION (AVG.±STD.DEV.) OF EVERY
STEP FOR EVERY SEGMENT

Step	Computational Proces	Time					
1-2	Acquisition of Raw Audio Segmentation of Clips into Segments	(5.22±0.14)ms					
	Segmentation of Segments into Frame Frame-Level Feature Extra	(47.05±0.42)ms					
3-7	Multiple Frames Accumu Dimension Reduction (LDA)	$(36.23\pm0.63)$ ms $(0.09\pm0.01)$ ms $(0.08\pm0.01)$ ms					
	Recognition of Raindrops Hitting on Umbrella	Train Test	<0.01ms				
	Total	(88.51±0.68)ms					

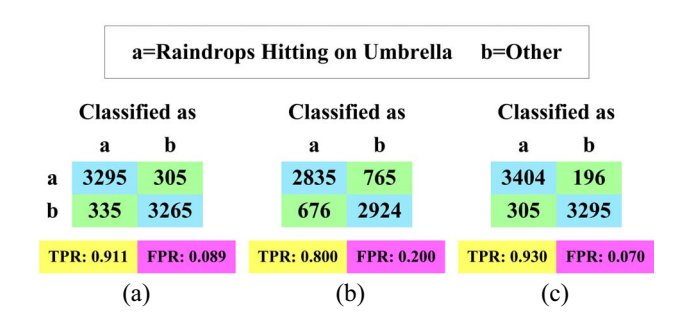


Fig. 9. In recognition of raindrops hitting on umbrella. Confusion matrices, TPR, and FPR of different recognition algorithms. (a) DT. (b) PCA + DT. (c) LDA + DT.

principal component analysis (PCA) and LDA. Fig. 9 presents the confusion matrices, TPR and FPR of these recognizers.

When comparing the performance of combining PCA and LDA with DT, we find out that LDA shows better performance. More detailed, LDA reduces the features to one dimension and only misrecognize 501 segments, while PCA reduces the

a=Light Rain b=Moderate Rain c=Heavy Rain																							
Classified as				Classified as				Classified as				Classified as				Classified as				Classified as			
	a	b	c		a	b	e		a	b	c		a	b	c		a	b	c		a	b	c
a	1109	60	31		1121	59	20		1111	59	30		1112	62	26		1100	82	18		1105	78	17
b	52	1096	52		54	1113	33		57	1073	70		50	1086	64		55	1107	38		36	1125	39
c	23	33	1144		15	37	1148		191	108	901		13	59	1128		14	34	1152		17	83	1100
		(a)				(b)				(c)				(d)				(e)				(f)	

Fig. 10. In measurement of rain. Confusion matrices of different classifiers.

features to three dimensions (account for 98% of the eigenvalues) and misrecognize 1441 segments. In addition, the TPR of the combination of LDA and DT is 93.0%, which outperforms the original DT algorithm by 1.9%. However, the combination of PCA and DT shows worse performance than the original DT and only achieves 80.0% TPR.

## C. Measurement of Rain

In this section, we examine how well Chaac can measure the coarse rain intensity, namely, light, moderate and heavy rain, based on segments generated by raindrops hitting on umbrella utilizing six different classification algorithms. Our experimental dataset contains 1200 light rain, 1200 moderate rain and 1200 heavy rain segments in total.

1) Acquisition of Labeled Data: The rain intensity is quantified by the amount of rain per unit time. On the one hand, all of our experimental data are opportunistically crowdsourced by the participants in their daily lives. It is not only unreasonable but also unrealistic to ask every participant to carry a rain gauge with her all the time, which is cumbersome, as well as fragile. On the other hand, in order to save energy consumption, which can be negligible finally, every data collection process only lasts for 10 s. Obviously, it is impossible to measure the accurate amount of rain within such a short period of time. Then how about prolonging every data collection process to 10 or 30 min? Unfortunately, even during the time span of such order of magnitude, the accumulated rain is still too little to be measured, especially for light rain, while the rain intensity may have already changed several times. Actually, the amount of rain released to the public by professional meteorological department usually is a cumulative value within at least a day, a month or even a year. So the accurate short-time rain intensity is extremely hard to obtain, not only for us, but also for professional meteorological department. Due to the above two reasons, we only require every participant to label current rain intensity as light, moderate or heavy rain according to his or her observation. In order to improve the accuracy, we have uniformly trained all participants in advance, to unify the standard as far as possible.

2) Experimental Results: We build six recognizers based on different classification algorithms, respectively, DT, RF, naive Bayes (NB), multilayer perceptron, k-nearest neighbors (k-NNs), and support vector machine (SVM), and run tenfold cross-validation to evaluate their performance. In Fig. 10, we present the confusion matrices of the recognizers. We also illustrate the TPR and FPR of the recognizers in

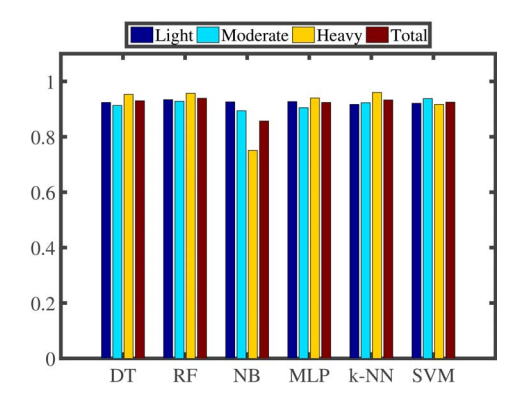


Fig. 11. In measurement of rain. TPR of different classifiers.

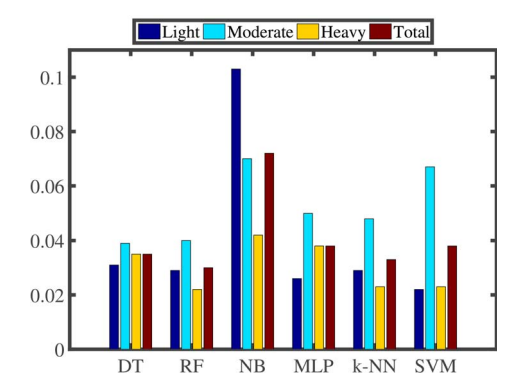


Fig. 12. In measurement of rain. FPR of different classifiers.

Figs. 11 and 12. At last, we compare the time consumption of six recognizers in Fig. 13.

We can make two main observations here. First, as presented in Figs. 10–12, RF outputs the best classification performance, namely, 93.9% TPR, 3.0% FPR, and 218 misclassification segments, *k*-NN achieves the second best classification performance and NB yields the worst classification performance, that is, 85.7% TPR, 7.2% FPR, and 515 misclassification segments. Second, we show the training time, test time and total time when running each classifier in Fig. 13. However, we only pay attention to the time consumption of the test process since the training process is accomplished before deploying the applications to the smartphones. Then we find out that *k*-NN is the most time-consuming algorithm which spends 0.86 s on testing 3600 labeled rain segments in our experimental dataset. In addition, SVM spends 0.44 s and other four algorithms can all be completed within 0.03 s.

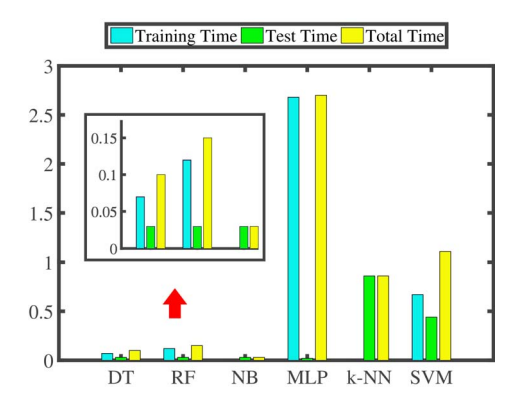


Fig. 13. In measurement of rain. Total time consumed of different classifiers.

#### D. Real World Evaluation

Finally, we evaluate how well Chaac can detect and measure the rain in real world. We choose the data at 6 P.M., on August 22, 2015, from our database and visualize them in Fig. 14, according to their real location information. This area is 11-km long and 3-km wide. We can observe that, currently, there are 21 participants in this area. A list of icons and their meanings is presented in Fig. 14(top). Each smartphone stands for a participant. We provide the ground truth of current point in geography on each smartphone, which is colored in black. From left to right, the first icon means whether it is clear or rainy at this point right now. The second icon, if any, denotes whether current audio clip is generated by raindrops hitting on umbrella or other sources, such as vehicles passing by. The third icon, if there is, indicates the current rain intensity right here. We present the recognition results, output by Chaac, of current position on the right side of each smartphone, which are based on ten consecutive 1-s long audio segments. The right results are colored in cyan and wrong in magenta. Among all the smartphones of our 21 participants, only two output the wrong results, which did not detect the rain. There are another two smartphones whose audio clips are generated by the moving vehicles, rather than the raindrops hitting on umbrella. Chaac has correctly recognized that, but cannot further measure the rain intensities of these two locations. The current rain information released by the CMA and nine other popular weather apps mentioned above are given in Fig. 14(bottom). On the one hand, there are as many as six apps even claim that it is a clear day in this area. This is because the rain comes very suddenly and these apps do not have time to update the data in time. By contrast, Chaac can detect and measure the rain in real time, which is accurate to each point in time dimension. On the other hand, as for the CMA as well as all of these nine weather apps mentioned above, some of them can at most be accurate to district-level, while the others can achieve up to city-level.<sup>2</sup> However, the experimental area in Fig. 14 is smaller than a district, but we can observe that the rain intensities differ greatly from west to east. It is raining heavily in the west, moderately and lightly in the middle, but it is totally clear in the east. So these weather apps can only provide the rain information of a very large area, which is not precise and practical enough. By contrast, Chaac can detect and measure the rain in fine granularity, which is accurate to each point in geography. In conclusion, Chaac is, to some extent, superior to other existing rain detection and measurement methods.

#### VI. DISCUSSION

## A. Privacy Issues

The users' privacy, which we believe is the matter with the highest priority, should be strictly protected at any time and without conditions. There are four aspects we want to specify about the privacy issues related to Chaac. First, the application scenarios of Chaac are mainly outdoors, which are essentially open environments and thus much less sensitive in comparison with the scenes explored in some other previous acoustics-based related researches (e.g., in bedroom [11] and bathroom [6]). Second, in Chaac, human voices are not our concern at all and interestingly, exactly on the contrary, human voices interfere with the acoustical signals we really focus on and want to recognize. As for Chaac, human voices are, to some extent, noises. Third, Chaac does not store or transmit any raw audio data, which are all buffered and processed locally and offline on smartphones in real time and erased immediately after feature extraction. Chaac only reports the recognition results, namely, clear or rainy day as well as light, moderate or heavy rain, to achieve crowdsourcing. Fourth, Chaac empowers users to completely control all raw audio data collected, that is to say, users are allowed to delete any or even purge all of their data and pause the raw audio data acquisition process for any upcoming time intervals or at any certain locations through the user interfaces of Chaac.

## B. Motivation Issues

Recently, the surge in popularity of crowdsourcing attracts a large number of researchers, who have conducted massive, systematic and thorough studies of its fundamental mechanisms, including the motivation, that is to say, how to encourage people to share their high-quality data. Researches in this area include [4], [5], [12], [15], and so on. These previous research achievements can be directly applied to our scenario toward rain detection and measurement. To say the least, even without these existing work mentioned above, the motivation of people in this paper is still obvious. People take part in the rain monitoring process, only then can they use the rain information shared by other people, which is a win-win situation. Thus, the motivation of people is not an important problem for us, so it is beyond the scope of this paper.

In what follows, we look ahead to some future research directions.

#### C. Remaining Meteorological Phenomena

The detection and measurement of snow, thunder and other less common meteorological phenomena, such as hail, hurricane and sandstorm, are beyond the scope of this paper. In future, we will endeavor to add these functions to Chaac to make it more practical. The methodologies are similar, for example, as for snow and hail scenarios, we find that there are also a variety of obvious acoustic clues (e.g., "creak"

<sup>&</sup>lt;sup>2</sup>A city usually consists of several districts.

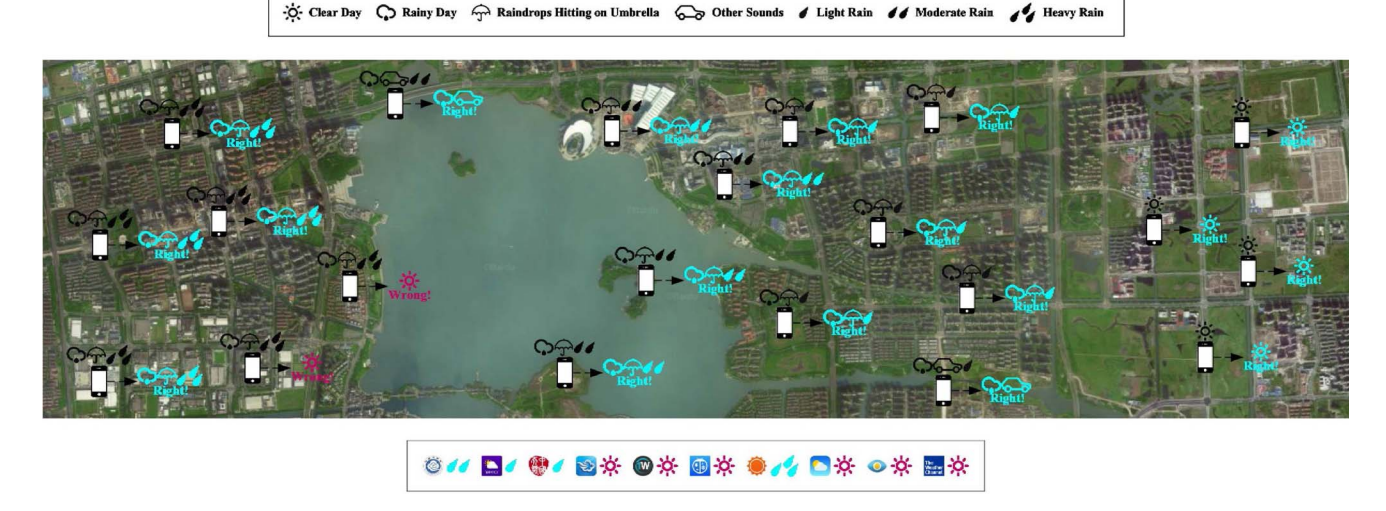


Fig. 14. Comparison among the rain detection and measurement results output by Chaac in real world, the rain information released by the CMA and nine other popular weather apps, to show that Chaac is real-time and fine-grained.

emitted when pedestrians walk and vehicles move on accumulated snow and "rat-a-tat" generated when hailstones hit against windows, ground, and roofs of vehicles correspondingly). Consequently, exploiting these acoustic hints ulteriorly will be considered as our further work.

#### VII. CONCLUSION

In this paper, we present a rain detection and measurement system, namely Chaac, which exploits opportunistically crowdsourced audio clips from smartphones. In the implementation of Chaac, three dedicated processing parts are performed. In the beginning, Chaac detects whether it is raining. If it is raining, Chaac will try to ulteriorly judge whether the current audio clip is generated by raindrops hitting on the umbrella. Finally, Chaac measures current rain intensity in real time. To achieve these three parts above, we cannily extract and refine a series of features and then construct several supervised classifiers. The experiments results show that Chaac can detect and measure the rain accurately, which brings rain observations with high temporal and spatial resolution technologically and economically within reach.

#### REFERENCES

- [1] P. Allamano, A. Croci, and F. Laio, "Toward the camera rain gauge," Water Resources Res., vol. 51, no. 3, pp. 1744–1757, 2015.
- [2] T. Bellerby, M. Todd, D. Kniveton, and C. Kidd, "Rainfall estimation from a combination of TRMM precipitation radar and GOES multispectral satellite imagery through the use of an artificial neural network," *J. Appl. Meteorol.*, vol. 39, no. 12, pp. 2115–2128, 2000.
- [3] M. Z. A. Bhuiyan, G. Wang, J. Cao, and J. Wu, "Sensor placement with multiple objectives for structural health monitoring," ACM Trans. Sensor Netw., vol. 10, no. 4, p. 68, 2014.
- [4] D. C. Brabham, "Moving the crowd at threadless: Motivations for participation in a crowdsourcing application," *Inf. Commun. Soc.*, vol. 13, no. 8, pp. 1122–1145, 2010.
- [5] D. Chandler and A. Kapelner, "Breaking monotony with meaning: Motivation in crowdsourcing markets," *J. Econ. Behav. Organ.*, vol. 90, pp. 123–133, Jun. 2013.
- [6] J. Chen, A. H. Kam, J. Zhang, N. Liu, and L. Shue, "Bathroom activity monitoring based on sound," in *Proc. ICPC*, Munich, Germany, 2005, pp. 47–61.

- [7] S. Görmer, A. Kummert, S.-B. Park, and P. Egbert, "Vision-based rain sensing with an in-vehicle camera," in *Proc. IEEE IV*, 2009, pp. 279–284.
- [8] D. I. F. Grimes and M. Diop, "Satellite-based rainfall estimation for river flow forecasting in Africa. I: Rainfall estimates and hydrological forecasts," *Hydrol. Sci. J.*, vol. 48, no. 4, pp. 567–584, 2003.
- [9] H. Guo et al., "Tefnut: An accurate smartphone based rain detection system in vehicles," in Proc. WASA, 2016, pp. 13–23.
- [10] U. Haberlandt and M. Sester, "Areal rainfall estimation using moving cars as rain gauges—A modelling study," *Hydrol. Earth Syst. Sci.*, vol. 14, no. 7, pp. 1139–1151, 2010.
- [11] T. Hao, G. Xing, and G. Zhou, "iSleep: Unobtrusive sleep quality monitoring using smartphones," in *Proc. ACM SenSys*, 2013, p. 4.
- [12] H. Huang, X.-Y. Li, Y.-E. Sun, H. Xu, and L. Huang, "PPS: Privacy-preserving strategyproof social-efficient spectrum auction mechanisms," *IEEE Trans. Parallel Distrib. Syst.*, vol. 26, no. 5, pp. 1393–1404, Mar. 2015.
- [13] Z. Jiang et al., "VADS: Visual attention detection with a smartphone," in Proc. IEEE INFOCOM, 2016, pp. 1–9.
- [14] A. Kamilaris and A. Pitsillides, "Mobile phone computing and the Internet of Things: A survey," *IEEE Internet Things J.*, vol. 3, no. 6, pp. 885–898, Dec. 2016.
- [15] N. Kaufmann, T. Schulze, and D. Veit, "More than fun and money. Worker motivation in crowdsourcing—A study on mechanical turk," in *Proc. AMCIS*, vol. 11, 2011, pp. 1–11.
- [16] C. Kidd et al., "So, how much of the earth's surface is covered by rain gauges?" Bull. Amer. Meteorol. Soc., vol. 98, no. 1, pp. 69–78, 2017.
- [17] H. Leijnse, R. Uijlenhoet, and J. N. M. Stricker, "Rainfall measurement using radio links from cellular communication networks," *Water Resources Res.*, vol. 43, no. 3, pp. 1–6, 2007.
- [18] H. Li, H. Zhu, S. Du, X. Liang, and X. S. Shen, "Privacy leakage of location sharing in mobile social networks: Attacks and defense," *IEEE Trans. Depend. Secure Comput.*, vol. 15, no. 4, pp. 646–660, Jul./Aug. 2018.
- [19] H. Li, H. Zhu, and D. Ma, "Demographic information inference through meta-data analysis of Wi-Fi traffic," *IEEE Trans. Mobile Comput.*, vol. 17, no. 5, pp. 1033–1047, May 2018.
- [20] J. Wang, Z. Li, M. Li, Y. Liu, and Z. Yang, "Sensor network navigation without locations," in *Proc. IEEE INFOCOM*, Apr. 2009, pp. 2419–2427.
- [21] Y. Li, L. Zhou, H. Zhu, and L. Sun, "Privacy-preserving location proof for securing large-scale database-driven cognitive radio networks," *IEEE Internet Things J.*, vol. 3, no. 4, pp. 563–571, Aug. 2016.
- [22] Z. Li, M. Li, P. Mohapatra, J. Han, and S. Chen, "iType: Using eye gaze to enhance typing privacy," in *Proc. IEEE INFOCOM*, 2017, pp. 1–9.
- [23] Z. Liu, S. Jiang, P. Zhou, and M. Li, "A participatory urban traffic monitoring system: The power of bus riders," *IEEE Trans. Intell. Transp. Syst.*, vol. 18, no. 10, pp. 2851–2864, Oct. 2017.

[24] F. Nashashibi, R. de Charrette, and A. Lia, "Detection of unfocused raindrops on a windscreen using low level image processing," in *Proc. IEEE ICARCV*, 2010, pp. 1410–1415.

- [25] G. Peeters, "A large set of audio features for sound description (similarity and classification) in the CUIDADO project," IRCAM, Paris, France, Rep., 2004.
- [26] A. Rayitsfeld, R. Samuels, A. Zinevich, U. Hadar, and P. Alpert, "Comparison of two methodologies for long term rainfall monitoring using a commercial microwave communication system," *Atmos. Res.*, vols. 104–105, pp. 119–127, Feb. 2012.
- [27] D. A. Reynolds, T. F. Quatieri, and R. B. Dunn, "Speaker verification using adapted Gaussian mixture models," *Digit. signal Process.*, vol. 10, nos. 1–3, pp. 19–41, 2000.
- [28] D. A. Reynolds and R. C. Rose, "Robust text-independent speaker identification using Gaussian mixture speaker models," *IEEE Trans. Speech Audio Process.*, vol. 3, no. 1, pp. 72–83, Jan. 1995.
- [29] M. Roser and A. Geiger, "Video-based raindrop detection for improved image registration," in *Proc. IEEE ICCV (ICCV Workshops)*, 2009, pp. 570–577.
- [30] M. Shahzad and A. X. Liu, "Fast and accurate tracking of population dynamics in RFID systems," in *Proc. IEEE ICDCS*, 2017, pp. 836–846.
- [31] M. Shahzad, A. X. Liu, and A. Samuel, "Secure unlocking of mobile touch screen devices by simple gestures: You can see it but you can not do it," in *Proc. ACM MobiCom*, 2013, pp. 39–50.
- [32] L. Shangguan, Z. Yang, A. X. Liu, Z. Zhou, and Y. Liu, "STPP: Spatial-temporal phase profiling-based method for relative RFID tag localization," *IEEE/ACM Trans. Netw.*, vol. 25, no. 1, pp. 596–609, Feb. 2017.
- [33] F. Tapiador, R. Checa, and M. De Castro, "An experiment to measure the spatial variability of rain drop size distribution using sixteen laser disdrometers," *Geophys. Res. Lett.*, vol. 37, no. 16, pp. 1–6, 2010.
- [34] G. Wang et al., "Verifiable smart packaging with passive RFID," in Proc. ACM Ubicomp, 2016, pp. 156–166.
- [35] T. Wardah, S. H. A. Bakar, A. Bardossy, and M. Maznorizan, "Use of geostationary meteorological satellite images in convective rain estimation for flash-flood forecasting," *J. Hydrol.*, vol. 356, nos. 3–4, pp. 283–298, 2008.
- [36] M. Xiao, J. Wu, L. Huang, Y. Wang, and C. Liu, "Multi-task assignment for crowdsensing in mobile social networks," in *Proc. IEEE INFOCOM*, Apr. 2015, pp. 2227–2235.
  [37] B. Xie *et al.*, "LIPS: A light intensity–based positioning system for
- [37] B. Xie et al., "LIPS: A light intensity-based positioning system for indoor environments," ACM Trans. Sensor Netw., vol. 12, no. 4, p. 28, 2016.
- [38] L. Xie et al., "Tell me what i see: Recognize RFID tagged objects in augmented reality systems," in Proc. ACM Ubicomp, 2016, pp. 916–927.
- [39] A. Yatagai et al., "APHRODITE: Constructing a long-term daily gridded precipitation dataset for Asia based on a dense network of rain gauges," Bull. Amer. Meteorol. Soc., vol. 93, no. 9, pp. 1401–1415, 2012.
- [40] P. Zhou, Y. Zheng, Z. Li, M. Li, and G. Shen, "IODetector: A generic service for indoor outdoor detection," in *Proc. ACM Sensys*, 2012, pp. 113–126.
- [41] Z. Zhou, L. Shangguan, X. Zheng, L. Yang, and Y. Liu, "Design and implementation of an RFID-based customer shopping behavior mining system," *IEEE/ACM Trans. Netw.*, vol. 25, no. 4, pp. 2405–2418, Aug. 2017.
- [42] A. Zinevich, H. Messer, and P. Alpert, "Frontal rainfall observation by a commercial microwave communication network," J. Appl. Meteorol. Climatol., vol. 48, no. 7, pp. 1317–1334, 2009.
- [43] Z. Zivkovic, "Improved adaptive Gaussian mixture model for background subtraction," in *Proc. IEEE ICPR*, vol. 2, 2004, pp. 28–31.



Hansong Guo received the B.E. degree in computer science and technology from the University of Science and Technology of China, Hefei, China, in 2013. He is currently pursuing the Ph.D. degree in computer science and technology at the University of Science and Technology of China, and the joint Ph.D. degree at the University of Florida, Gainesville, FL, USA, under the supervision of Prof. L. Huang and Prof. S. Chen.

His current research interests include ubiquitous computing, mobile sensing, and big data analysis,

most of which focus on utilizing signal processing and machine learning to develop new technologies at the frontier of mobile systems.



**He Huang** (M'16) received the Ph.D. degree in computer science and technology from the University of Science and Technology of China, Hefei, China, in 2011

He is currently an Associate Professor with the Department of Computer Science and Technology, Soochow University, Suzhou, China. His current research interests include network traffic measurement, spectrum auction, privacy preserving, crowdsourcing, software-defined networks, and satellite networks.



**Yu-E Sun** received the Ph.D. degree in computer science and technology from the Shenyang Institute of Computing Technology, Chinese Academy of Sciences, Shenyang, China, in 2011.

She is currently an Associate Professor with the Department of Urban Rail Transportation, Soochow University, Suzhou, China. Her current research interests include network traffic measurement, spectrum auction, privacy preserving, and wireless networks.



Youlin Zhang received the B.E. degree in electronic information engineering from the University of Science and Technology of China, Hefei, China, in 2014. He is currently pursuing the Ph.D. degree in computer and information science and engineering at the University of Florida, Gainesville, FL, USA, under the supervision of Prof. S. Chen.

His current research interests include next generation RFID technologies and Internet of Things.



Shigang Chen (A'03–M'04–SM'12–F'16) received the B.S. degree in computer science from the University of Science and Technology of China, Hefei, China, in 1993, and the M.S. and Ph.D. degrees in computer science from the University of Illinois at Urbana–Champaign, Champaign, IL, USA, in 1996 and 1999, respectively.

He joined the University of Florida, Gainesville, FL, USA, as an Assistant Professor in 2002, and became an Associate Professor in 2008 and a Professor in 2013. He is currently a Professor with

the Department of Computer and Information Science and Engineering, University of Florida. He was with Cisco Systems, San Jose, CA, USA, where he was involved with network security for three years and helped start a network security company, Protego Networks, Sunnyvale, CA, USA. He has authored or co-authored over 190 peer-reviewed journal/conference papers and holds 12 U.S. patents.

Prof. Chen was a recipient of the IEEE Communications Society Best Tutorial Paper Award in 1999, the NSF CAREER Award in 2007, the Cisco University Research Award in 2007 and 2012, the University of Florida Research Foundation Professorship for the year 2017–2020, and the University of Florida Term Professorship for the year 2017–2020. He is an ACM Distinguished Member and an IEEE ComSoc Distinguished Lecturer.



Liusheng Huang received the M.S. degree in computer science and technology from the University of Science and Technology of China, Hefei, China, in 1988

He is a Professor and a Doctoral Advisor with the Department of Computer Science and Technology, University of Science and Technology of China, where he is currently the Vice Dean of the Suzhou Institute for Advanced Study. He has authored over 180 conference papers, over 110 international journal papers, over 120 Chinese journal papers, and

over 6 books. His current research interests include wireless sensor networks, Internet of Things, Internet of Vehicles, secure multiparty computation, information security, cloud security as well as big data analysis and privacy preserving.

Mr. Huang was a recipient of the Special Government Allowance of the State Council of the China. He has served as the Chair or as a Technical Program Committee member for many prestigious international conferences.